Robust control with an anti-windup technique based in relaxed LMI conditions for LTV system

Rosana Rego*

Federal University of Rio Grande do Norte,
Natal, RN, 59077080, Brazil
Email: rosana.rego@ufersa.edu.br
*Corresponding author

Marcus Costa

Department of Engineering,
Federal Rural University of the Semi-Arid,
59780000, Caraúbas, RN, Brazil
Email: marcus.costa@ufersa.edu.br

Abstract: This paper proposes a new technique to address the anti-windup (AW) with model predictive control (MPC) scheme for linear time-varying (LTV) systems. The main advantage of this new approach is the reduced conservativeness compared with other well-known anti-windup techniques and to prevent integration windup in MPC controllers when the actuators are saturated. The control with AW is applied in a three-state switching cell (3SSC) DC-DC converter operating under saturation conditions. The MPC with proposed anti-windup is compared with the MPC technique and with MPC-AW without relaxation. The MPC-AW with relaxation improves the performance when the converter operated in the saturated mode and allows the rational use of the converter. The simulation results validated the efficiency of the proposed approach and showed that the proposed approach not only allows working better with the polytope modeling but also improves the response under LTV disturbance.

Keywords: anti-windup; MPC; model predictive control; boost converter; linear time-varying systems; linear matrix inequalities; DC-DC converter; boost converter; LTV disturbance; 3SSC converter.

Biographical notes: Rosana Rego received her BS in Science and Technology (2015) and a BS in Computer Engineering from the Federal Rural University of the Semi-Arid (2017). Master in Electrical Engineering from the Federal Rural University of the Semi-Arid (2019). Currently a PhD student in Electrical Engineering at the Federal University of Rio Grande do Norte, with research in the area of Intelligent Control, Neural control, neural networks.

Marcus Costa received his BS in Electrical Engineering from the Federal University of Ceará (2009), and Master's degree in Electrical Engineering from the Federal University of Ceará (2012) and a PhD in Electrical Engineering from the Federal University of Ceará (2017). He is currently a Professor of higher education at the Federal Rural University of the Semi-Arid.

1 Introduction

Anti-windup (AW) techniques are used to prevent the plant's control signal from entering the saturation region. In practice, the control signal can have a different value from the signal that actually acts on the plant, i.e., the control signal stays at the saturation region, which is not desired because deterioration of system performance occurs. This phenomenon is known as windup (Qi et al., 2018; Turner et al., 2003; Rego and Costa, 2020; Rego et al., 2018). In this way, the windup is an unwanted effect. Hence, in the last two decades, the problem

of designing the anti-windup compensator that guarantees closed-loop stability and satisfies certain performance criteria has been extensively explored (De Doná et al., 2000; Turner et al., 2003; Ran et al., 2016; Wada and Saeki, 2016; Fang et al., 2018; Rego et al., 2018; Errouissi and Al-Durra, 2018; Su et al., 2016; Zheng et al., 2019). De Doná et al. (2000) discuss the relationship between the AW technique and the model predictive control (MPC), in which the AW control considered in the work is based on the law of closed-loop control with state saturation applied to LTV system. Wada and Saeki (2016) shows a method of designing an anti-windup

compensator with the MPC control for a system with input restrictions. Ran et al. (2016) proposes the application of AW in uncertain systems. And Fang et al. (2018) presents results on a dynamic anti-windup compensator for the flexible AC transmission system-based wide-area damping controller.

Papers with the anti-windup technique applied to converters that we can mention are Rego and Costa (2020), Rego et al. (2018), Huang et al. (2004), Tomaszewski and Jiangy (2016) and Tarczewski et al. (2017). Huang et al. (2004) presents analysis and design of a high-power multileg interleaved boost converter and tests different anti-windup schemes for a typical PI-controller are evaluated. Rego et al. (2018) presents the MPC control with anti-windup compensator (AW) optimised via LMIs for boost converter control. Errouissi and Al-Durra (2018) proposes a novel decoupled PI current controller for grid-tied inverters with an anti-windup scheme arises naturally into the controller, leading to an improved transient performance in the presence of saturation. And Tarczewski et al. (2017) presented a gain-scheduled constrained state feedback controller for a SiC MOSFET direct current DC-DC buck power converter with a non-synchronous control strategy with anti-windup to avoid the windup phenomenon.

Hence, it can be observed that applications of robust controllers with anti-windup compensators are still incipient for studies related to static converters (Rego et al., 2018; Tomaszewski and Jiangy, 2016). These converters are widely used in power supply systems. One of the converters of interest, mainly in the area of power electronics are the boost converters (Costa et al., 2017). The purpose of these converters is to provide a DC voltage output even when subjected to load or input voltage variations (Guldemir, 2011). Although it has a simplified topology, it presents some singularities in its modelling, such as variations of load resistance and input voltage (Linares-Flores et al., 2014; Ortega et al., 2013). And realising the control of these converters is considered a complicated task due to their singularities (Amirifar, 2005). The windup on converters can be modelled as the overlapping effect. This effect occurs when the control signal operates in a region such that there is simultaneous conduction of two or more offset keys (Rego et al., 2018).

Thus, in this work we propose an improvement in AW technique of Herrmann et al. (2003) based on procedures of Cuzzola et al. (2002) and Wada et al. (2006). The improvement reduces the conservatism of a convex hull without the loss of feasibility properties while enhancing the control performance.

The AW technique was implemented with the MPC discussed in Costa et al. (2017); Rego et al. (2018). It was decided to control the boost converter with the MPC control technique because the MPC proved to be a very robust control type in most applications, such as in static converters and in electric drive devices. The main causes of this control are that it can be applied either to linear or non-linear multivariate (Camacho and Alba, 2013; Aguirre et al., 2007; Costa et al., 2017; Ma and Fang, 2019). And works using offline MPC with uncertain models have increased in the last years as seen in Paulson et al. (2017), Lorenzen et al. (2017), Zheng et al. (2018), Moradi et al. (2019), Hu and Ding (2019), Ping (2017) and Longge and Yan (2017).

Therefore, the new AW approach with MPC is applied to the control of three-state switching cell (3SSC) DC-DC boost converter with uncertainties operating under saturation conditions in the control signal. The uncertainties of the boost converter considered in this study are the load resistance and the input voltage. The major contribution of the research is that the proposed method improves the performance when the converter is operated in the saturated, and this allows the rational use of the converter, avoiding that the saturation damages its performance in a permanent regime. The benefit of this approach is demonstrated in the numerical simulation.

2 Boost converter

Figure 1 shows the boost converter used (Bascopé and Barbi, 2000; Costa et al., 2017). This converter is characterised by the switching method optimised, thus guaranteeing a higher percentage yield in its operation (Costa et al., 2017).

Figure 1 Boost converter with three-state switching cell
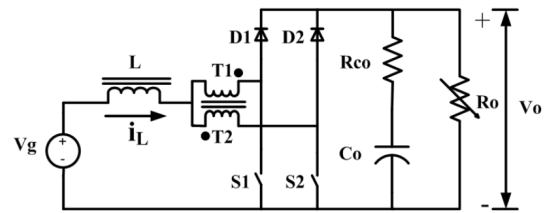
The boost converter in Figure 1 converts the input voltage range from 26V–36V to 48V with variable load from 380W–1000W. The parameters used for the converter is the same used by Rego and Costa (2020).

2.1 Mathematical modelling

The expressions in the state space A_t, B_t, C_t and D_t operating in continuous conduction mode (CCM) (Middlebrook and Cuk, 1976) are:

$$\dot{x} = A_t(t)x + B_t(t)u,$$
$$y = C_t(t)x + D_t(t)u,$$
(1)

where,

$$A_t = \begin{bmatrix} -\frac{(1-D_{cycle})(R_{co}\|R_o)}{L} & -\frac{(1-D_{cycle})R_o}{L(R_{co}+R_o)} \\ \frac{(1-D_{cycle})R_o}{C_o(R_{co}+R_o)} & -\frac{1}{C_o(R_{co}+Ro)} \end{bmatrix},$$
(2)

$$B_t = \frac{V_g}{R'} \begin{bmatrix} \frac{R_o}{L} \frac{(1-D_{cycle})R_o+R_{co}}{R_o+R_{co}} \\ -\frac{R_o}{R_o+R_{co}} \end{bmatrix},$$
(3)

$$C_t = \left[(1-D_{cycle})(R_{co}\|R_o) \frac{R_o}{R_{co}+R_o} \right],$$
(4)

$$D_t = -V_g \frac{R_{co}\|R_o}{R'}.$$
(5)

such that $R' = (1-D_{cycle})^2 R_o + D_{cycle}(1-D_{cycle})(R_{co}\|R_o)$, $x = [i_L\ V_c]^T$ where i_L is the inductor

current, V_c is capacitor voltage, u is the control signal, D_{cycle} is the duty cycle and $y = V_o$, V_o is the output voltage.

The uncertainties of the model can be defined by Costa et al. (2017):

$$R_o = f(Pot) = \frac{V_o^2}{Pot} \quad Pot \in [Pot_{min} \; Pot_{max}], \quad (6)$$

$$D_{cycle} = f(V_g) = 1 - \frac{V_g}{V_o} \quad V_g \in [V_{g_{min}} \; V_{g_{max}}]. \quad (7)$$

With this variation in input voltage V_g and load R_o, system becomes variant with uncertain parameters. Thus one way of representing this system is by using polytopic modelling. Therefore considering the equations, (7) and (6), system (1) belongs to the following polytope formed by the four local models,

$$[A_t(R_o, D_{cycle})), B_t(R_o, D_{cycle}), C_t(R_o, D_{cycle}),$$
$$D_t(R_o, D_{cycle})] \in Co\,\{[A_1, B_1, C_1, D_1], \quad (8)$$
$$[A_2, B_2, C_2, D_2], [A_3, B_3, C_3, D_3], \; [A_4, B_4, C_4, D_4]\},$$

where, $Co\{\cdot\}$ denotes the convex hull of the polytope and $[A_j, B_j, C_j, D_j]$ are vertices of the polytopic. In this way, system is time-varying with variations in power ($[Pot_{min} \; Pot_{max}]$) and input voltage ($[V_{g_{min}} \; V_{g_{max}}]$).

3   Problem statement

Figure 2 shows the proposed block diagram by Rego et al. (2018). A, B, C and D are the discretised matrices in state space. As seen in Figure 2 an integral action will be applied in the control signal, as proposed in Costa et al. (2017). Still in Figure 2 g, h are the matrices that correspond to the degree freedom of the integral action block diagram and v is the integral action. K_I and K are respectively the integral action gain and MPC control gain. $r(k)$ is the input reference of system, and $y(k)$ is the output of system.

The coprime matrices are given by,

$$\Theta(z) = \begin{bmatrix} M(z) - I \\ G(z)M(z) \end{bmatrix} \sim \left[\begin{array}{c|c} A + BF_{AW} & B \\ \hline F_{AW} & 0 \\ C + DF_{AW} & D \end{array} \right], \quad (9)$$

where F_{AW} is the anti-windup gain, and A, B, C and D are the discretised matrices of the boost converter. The expressions of the anti-windup actuator are defined by,

$$x_d(k+1) = (A + BF_{AW})x_d(k) + B\tilde{u}(k), \quad (10)$$

$$u_d(k) = F_{AW}x_d(k), \quad (11)$$

$$y_d(k) = (C + DF_{AW})x_d(k) + D\tilde{u}(k). \quad (12)$$

To calculate the anti-windup gain (Turner et al., 2003) proposes the Theorem 1.

Theorem 1 (Turner et al., 2003)**:** *propose that there is a discrete time dynamic compensator that solves the windup problem if and only if there exists a dynamic compensator $\Theta(z)$ of order n_p which solves strongly the anti-windup problem if there exist matrices $Q_a > 0$, $U_a = diag(\mu_1, ..., \mu_m)$, $L_a \in$*

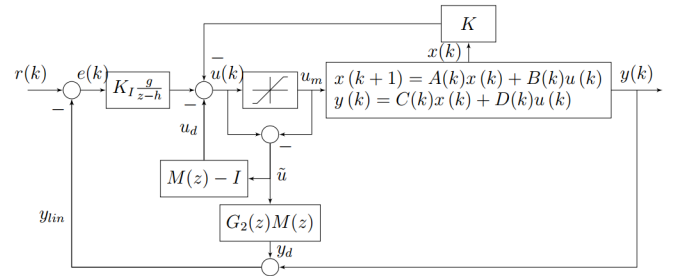$R^{(m+q) \times m}$ *and a scalar $\mu_a > 0$, such that the following linear matrix inequality is satisfied,*

$$\min \gamma_a$$
$$\begin{bmatrix} -Q_a & * & * & * & * \\ -L_a & -2U_a & * & * & * \\ 0 & I & -\mu_a I & * & * \\ (C_j Q_a + D_j L_a) & D_j U_a & 0 & -I & * \\ (A_j Q_a + B_j L_a) & B_j U_a & 0 & 0 & -Q_a \end{bmatrix} < 0. \quad (13)$$

Where $F_{AW} = L_a Q_a^{-1}$ is anti-windup action gain, based on coprime factorisation. And $\gamma_a = \sqrt{\mu_a}$.

Using this theorem, we can achieve an anti-windup gain to avoid the windup or overlapping effect on converters with uncertainties. But, due to the fact that the uncertainties present in system can lead to an infeasible problem when they are largely increased or modified. We will use a procedure that reduces the conservatism of a convex hull without the loss of feasibility properties while enhancing performance. A procedure used to enhance the feasibility problem of constraints is the LMI relaxation, as proposed by Cuzzola et al. (2002) and Wollnack et al. (2017)

Figure 2   Control diagram

3.1   Convex relaxation of anti-windup LMI

Theorem 2: *There exists a dynamic compensator $\Theta(z)$ of order n_p which solves strongly the anti-windup problem if there exist matrices $Q_a > 0$, $X_a \neq X_a^T$, $U_a = diag(\mu_1, ..., \mu_m)$, $L_a \in R^{(m+q) \times m}$ and a scalar $\mu_a > 0$, such that the following linear matrix inequality is satisfied,*

$$\begin{bmatrix} -(X_a + X_a^T - Q_{aj}) & * & * & * & * \\ -L_a & -2U_a & * & * & * \\ 0 & I & -\mu_a I & * & * \\ C_j X_a + D_j L_a & D_j U_a & 0 & -I & * \\ A_j X_a + B_j L_a & B_j U_a & 0 & 0 & -Q_{aj} \end{bmatrix} < 0. \quad (14)$$

where $j = 1, ..., p$, and the gain $F_{AW}(k) = L_a X_a^{-1}$.

Proof: See Appendix A.

With the matrix inequality (14), we obtain a faster response of system when the control signal enters the saturation region and reduces the conservatism of the convex hull.

3.2 Block diagram – model with integral action

The augmented matrices for system (1), without considering the anti-windup effects are given by,

$$\hat{A}_j = \begin{bmatrix} A_j & 0 \\ -hC_j & g \end{bmatrix}, \tag{15}$$

$$\hat{B}_j = \begin{bmatrix} B_j \\ -hD_j \end{bmatrix}, \tag{16}$$

$$\hat{C}_j = \begin{bmatrix} C_j & 0 \end{bmatrix}, \tag{17}$$

whose closed-loop expressions are given by,

$$\bar{A} = \begin{bmatrix} A_j - B_j K & B_j K_I \\ -h(C_j - D_j K) & g - hD_j K_I \end{bmatrix}, \tag{18}$$

$$\bar{B} = \begin{bmatrix} 0 \\ h \end{bmatrix}, \tag{19}$$

$$\bar{C} = \begin{bmatrix} (C_j - D_j K) & D_j K_I \end{bmatrix}, \tag{20}$$

$$\bar{D} = 0. \tag{21}$$

where $\bar{A}, \bar{B}, \bar{C}$ and $\bar{D}$ are the closed-loop matrices whose state is defined by,

$$\hat{x} = \begin{bmatrix} x(k) \\ v(k) \end{bmatrix}, \tag{22}$$

where $v(k)$ is the integral action.

3.3 MPC control

The formulation of the offline MPC used are given by the following inequalities, as proposed in Rego (2019); Rego et al. (2018); Wan and Kothare (2002),

$$\max_{\begin{bmatrix} \hat{A}(k+i) & \hat{B}(k+i) \end{bmatrix} \in \Omega,\, i \geq 0} J_\infty(k) \leq V(k+i|k) \leq \gamma$$

$$\begin{bmatrix} 1 & \hat{x}(k|k) \\ \hat{x}(k|k) & Q \end{bmatrix} \geq 0, \, Q > 0, \tag{23}$$

$$\begin{bmatrix} Q & * & * & * \\ \hat{A}_i Q + \hat{B}_i Y & Q & * & * \\ Q_c^{1/2} Q & 0 & \gamma I & * \\ R^{1/2} Y & 0 & 0 & \gamma I \end{bmatrix} \geq 0, \, i = 1, \ldots, L \tag{24}$$

$$\begin{bmatrix} X & Y \\ Y^T & Q \end{bmatrix} \geq 0, \, X_{rr} \leq u_{r,\max}^2, \, r = 1, 2, \ldots, n_u \tag{25}$$

$$\begin{bmatrix} Z & \hat{C}\left(\hat{A}_i Q + \hat{B}_i Y\right) \\ * & Q \end{bmatrix} \geq 0, \, Z_{rr} \leq y_{r,\max}^2,$$

$$r = 1, 2, \ldots, n_y \tag{26}$$

where, $F = YQ^{-1}$ is the gain. If the Lyapunov function exists, then the gain found is stable (Wan and Kothare, 2002; Costa et al., 2017).

4 Numerical simulation

In order to test and compare the effectiveness of the improved anti-windup with MPC technique, we used boost convert model described in Section 2. We implemented the control only with the MPC with the LMIs (23), (23), (24), (25), and (26). Also we implemented the control anti-windup defined by Theorem 1 with MPC. We also implemented the proposed control anti-windup defined by Theorem 2 with MPC.

The circuit implementation considered non-linear continuous modelling using the Runge Kutta 4th order method. The initial states of system (1) is assumed as $x = [38.4615 \; 26]^T$. The set reference voltage was $V_o = 48$ V. The maximum value of the control signal was $u_{max} = 0.5$ and the operating points of the converter is 380–1000 W for sample time $T_s = 1$ ms and simulation step of the $1\mu s$, we used $g = h = 1$.

Thus, considering the function $f(V_g, Pot)$, system (1) belongs to the following polytope formed by the four local discrete models,

- $f(36V, 1000W)$

$$A_1 = \begin{bmatrix} -0.2838 & -7.7479 \\ 0.0634 & -0.1137 \end{bmatrix}, B_1 = \begin{bmatrix} 580.4780 \\ 65.2800 \end{bmatrix},$$
$$C_1 = \begin{bmatrix} 0.0198 & 0.9886 \end{bmatrix}, D_1 = -0.7304. \tag{27}$$

- $f(26V, 1000W)$

$$A_2 = \begin{bmatrix} 0.0958 & -8.4507 \\ 0.0692 & 0.2660 \end{bmatrix}, B_2 = \begin{bmatrix} 851.9920 \\ 53.4470 \end{bmatrix},$$
$$C_2 = \begin{bmatrix} 0.0143 & 0.9886 \end{bmatrix}, D_2 = -1.0054. \tag{28}$$

- $f(36V, 380W)$

$$A_3 = \begin{bmatrix} -0.3102 & -7.9646 \\ 0.0652 & -0.1119 \end{bmatrix}, B_3 = \begin{bmatrix} 542.7340 \\ 68.8140 \end{bmatrix},$$
$$C_3 = \begin{bmatrix} 0.0199 & 0.9956 \end{bmatrix}, D_3 = -0.2802. \tag{29}$$

- $f(26V, 380W)$

$$A_4 = \begin{bmatrix} 0.0759 & -8.7329 \\ 0.0715 & 0.02873 \end{bmatrix}, B_4 = \begin{bmatrix} 814.2740 \\ 58.5880 \end{bmatrix},$$
$$C_4 = \begin{bmatrix} 0.0144 & 0.9956 \end{bmatrix}, D_4 = -0.3871. \tag{30}$$

The weighting matrices are

$$Q_c = \begin{bmatrix} 1 & 0 & 0 \\ 0 & 0.1 & 0 \\ 0 & 0 & 0.1 \end{bmatrix}, \text{ and } R = 0.1. \tag{31}$$

The *anti-windup* gain obtained with the Theorem 2 was,

$$F_{AW} = [-0.2598 \; 116.5783] \times 10^{-4}. \tag{32}$$

The *anti-windup* gain obtained with the Theorem 1 was,

$$F_{AW} = [-8.0071 \; 54.4034] \times 10^{-4}. \tag{33}$$

And the controller gain

$$F_j = [\underbrace{0.0119 \; -0.7312}_{K} \; \underbrace{-0.1019}_{K_I}] \times 10^{-2} \tag{34}$$

K_I and K are respectively the integral action gain and MPC control gain.

A step variation of the input voltage of $26V - 36V$ was made, at the time of $0.075s$ and $0.225s$, whose analysis interval was between $0s$ and $0.3s$, as shown in the Figure 3.

Figures 4 and 5 show the variation of the load (R_o) and power (Pot) applied in system simulation.

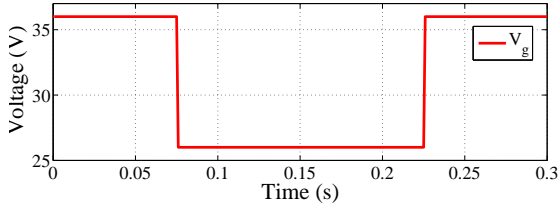**Figure 3**   Variation of the input voltage V_g (see online version for colours)

Figure 4   Variation of the load R_o (see online version for colours)
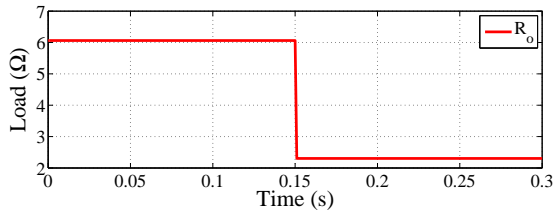

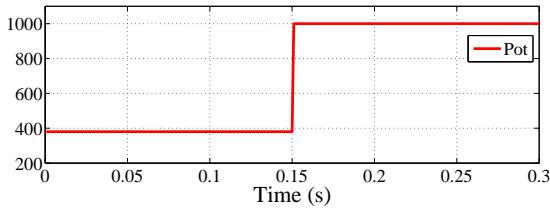**Figure 5**   Variation of the power Pot (see online version for colours)

Figure 6 shows the simulation results of the control signal limited by saturation $sat(u(k))$ and $u(k)$. It is noted that the control signal with actuator AW has a faster recovery than the circuit operating only with the MPC controller. In this way, the MPC-AW with relaxation improved performance when the converter operated in the saturated mode.

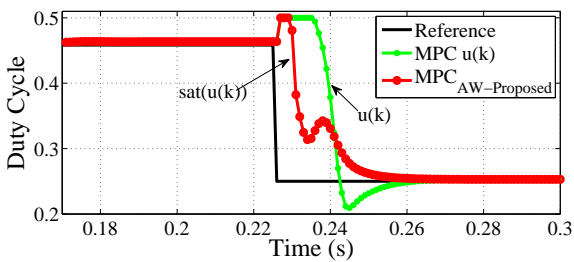**Figure 6** $sat(u(k))$ and $u(k)$ (see online version for colours)

Figure 7 shows the variation curve of the output voltage $y(k)$ in relation to the voltage variation of time. It is observed that system with actuator AW has a regimen recovery faster

than the circuit operating only with the MPC controller. The AW compensator produces a signal based on the difference between the controller output and the saturated actuator output, and then augment the signal to the control to deal with the windup phenomenon caused by actuator saturation.

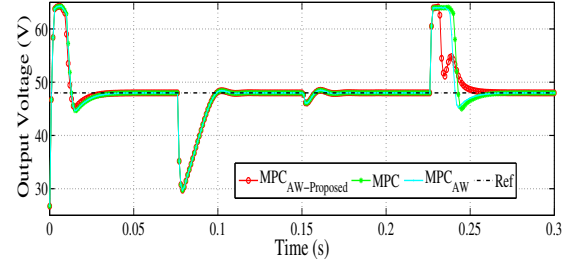**Figure 7**   Output voltage $y(k)$ (see online version for colours)

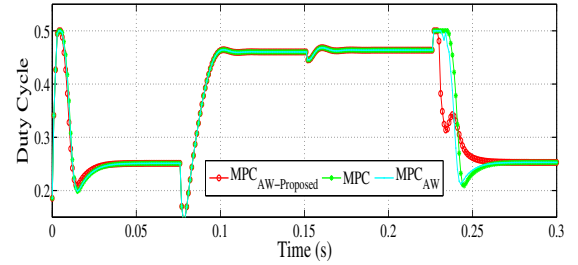**Figure 8**   Control signal $u(k)$ (see online version for colours)

Figure 9   Inductor current i_L (see online version for colours)
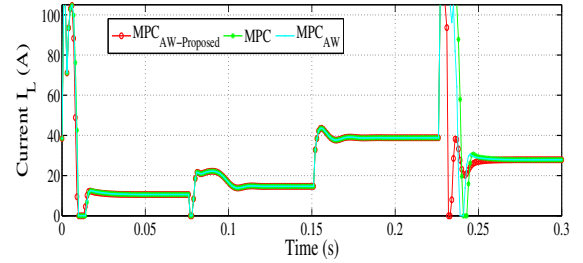

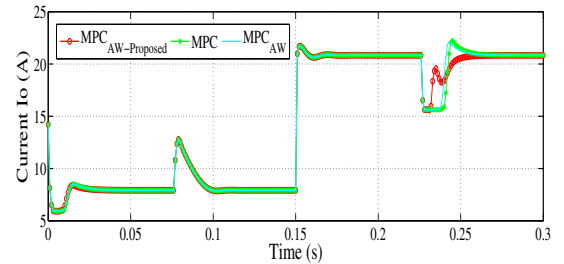**Figure 10**   Output current (see online version for colours)

Figure 8 shows the controller output $u(k)$. It respond almost immediately to changes in the setpoint. Without the anti-windup circuit (only with MPC), the responses is sluggish with delay. We can see that with LMI of relaxed anti-windup the response is even faster when compared with AW not relaxed. It is observed that the effect of the control signal of the proposed MPC-AW controller is reflected linearly in the inductor current (Figure 9) and in the output voltage (Figure 7). Similarly, the

control signal of the MPC controller is longer under saturation effect, impacting the responses of the current in the inductor and the output voltage.

In Figure 9 the current in the inductor has a situation similar to the output voltage. Scheme recovery of system with AW is faster than the model without AW. Even though all strategies reach an instantaneous peak current of about 105A, the proposed MPC-AW controller begins to act moments after reaching the peak current, different from the model controlled only by the MPC control, which only begins to act about 100 ms later.

Figure 10 shows the output current. Note how quickly the signal returns to the linear region and how fast the loop recovers from saturation at 0.225s with the proposed MPC-AW. Although MPC-AW method presents very good responses, as shown in Figures 7–10, our proposed method presents faster responses than MPC-AW without relaxation.

5 Conclusion

A new design method of an MPC with anti-windup structure for the boost converter is proposed. It has been shown in the numerical example that the proposed control system has a certain level of robustness. And the AW strategy applied in the operation of the control signal allows the rational use of the converter, avoiding that the saturation damages its performance in a permanent regime. The proposed approach not only allows working better with the polytope modelling but also improves the response under time-varying disturbance. The simulation results performed in the converter demonstrated that the proposed scheme is useful to suppress the actuator saturation. And the presented anti-windup method is simple, with a very low computational cost, and effective. In our future work, we intend to apply the obtained results to the real converter system and to extend the proposed method to parameter-varying system.

Acknowledgement

References

Aguirre, L.A., Bruciapaglia, A.H., Miyagi, P.E. and Piqueira, J. R.C. (2007) *Enciclopédia de automática: controle e automação*, Blucher.

Amirifar, R. (2005) 'Extended dynamic matrix control design for a dc-dc power converter', *Proceedings of the Thirty-Seventh Southeastern Symposium on System Theory, 2005. SSST'05*, IEEE, Tuskegee, AL, USA, pp.191–195.

Bascopé, G.T. and Barbi, I. (2000) 'Generation of a family of non-isolated dc-dc PWM converters using new three-state switching cells', *PESC 00. 2000 IEEE 31st Annual Power Electronics Specialists Conference, 2000*, Vol. 2, IEEE, pp.858–863.

Camacho, E.F. and Alba, C.B. (2013) *Model predictive control*, Springer, Science and Business Media.

Costa, M.V., Reis, F.E., Campos, J.C., Nogueira, F.G. and da Mota Almeida, O. (2017) 'Controlador robusto mpc-lmi aplicado ao conversor boost com célula de comutação de três estados', *Eletrônica de Potência*, Campo Grande, pp.81–90.

Cuzzola, F.A., Geromel, J.C. and Morari, M. (2002) 'An improved approach for constrained robust model predictive control', *Automatica*, Vol. 38, No. 7, pp.1183–1189.

De Doná, J.A., Goodwin, G.C. and Seron, M.M. (2000) 'Anti-windup and model predictive control: Reflections and connections', *European Journal of Control*, Vol. 6, No. 5, pp.467–477.

Errouissi, R. and Al-Durra, A. (2018) 'Decoupled pi current controller for grid-tied inverters with improved transient performances', *IET Power Electronics*, Vol. 12, No. 2, pp.245–253.

Fang, J., Yao, W., Chen, Z., Wen, J., Su, C. and Cheng, S. (2018) 'Improvement of wide-area damping controller subject to actuator saturation: a dynamic anti-windup approach', *IET Generation, Transmission and Distribution*, Vol. 12, No. 9, pp.2115–2123.

Guldemir, H. (2011) 'Modeling and sliding mode control of dc-dc buck-boost converter', *Proc. 6th Int. advanced technological Symp*, Vol. 4, pp.475–480.

Herrmann, G., Turner, M.C. and Postlethwaite, I. (2003) 'Discrete-time anti-windup: Part ii extension to the sampled-data case', *European Control Conference (ECC) 2003*, IEEE, Cambridge, UK, pp.479–484.

Hu, J. and Ding, B. (2019) 'An efficient offline implementation for output feedback min-max mpc', *International Journal of Robust and Nonlinear Control*, Vol. 29, No. 2, pp.492–506.

Huang, X., Wang, X., Nergaard, T., Lai, J-S., Xu, X. and Zhu, L. (2004) 'Parasitic ringing and design issues of digitally controlled high power interleaved boost converters', *IEEE Transactions on Power Electronics*, Vol. 19, No. 5, pp.1341–1352.

Linares-Flores, J., Mendez, A.H., Garcia-Rodriguez, C. and Sira-Ramirez, H. (2014) 'Robust nonlinear adaptive control of a boost converter via algebraic parameter identification', *IEEE Transactions on Industrial Electronics*, Vol. 61, No. 8, pp.4105–4114.

Longge, Z. and Yan, Y. (2017) 'Robust shrinking ellipsoid model predictive control for linear parameter varying system', *PLOS ONE*, Vol. 12, No. 6, pp.e0178625.

Lorenzen, M., Dabbene, F., Tempo, R. and Allgöwer, F. (2017) 'Stochastic mpc with offline uncertainty sampling', *Automatica*, Vol. 81, pp.176–183.

Ma, X. and Fang, S. (2019) 'Towards improving constrained robust model predictive control with free control moves', *International Journal of Modelling, Identification and Control*, Vol. 33, No. 3, pp.208–215.

Middlebrook, R. and Cuk, S. (1976) 'A general unified approach to modelling switching-converter power stages', *Power Electronics Specialists Conference, 1976 IEEE*, IEEE, Cleveland, OH, USA, pp.18–34.

Moradi, S.M., Akbari, A. and Mirzaei, M. (2019) 'An offline LMI-based robust model predictive control of vehicle active suspension system with parameter uncertainty', *Transactions of the Institute of Measurement and Control*, Vol. 41, No. 6, pp.1699–1711.

Ortega, R., Perez, J. A.L., Nicklasson, P.J. and Sira-Ramirez, H.J. (2013) *Passivity-Based Control of Euler-Lagrange Systems: Mechanical, Electrical and Electromechanical Applications*, Springer Science and Business Media.

Paulson, J.A., Xie, L. and Mesbah, A. (2017) 'Offset-free robust mpc of systems with mixed stochastic and deterministic uncertainty', *IFAC-PapersOnLine*, Vol. 50, No. 1, pp.3530–3535.

Ping, X. (2017) 'Output feedback robust mpc based on off-line observer for lpv systems via quadratic boundedness', *Asian Journal of Control*, Vol. 19, No. 4, pp.1641–1653.

Qi, W., Park, J.H., Zong, G., Cao, J. and Cheng, J. (2018) 'Anti-windup design for saturated semi-Markovian switching systems with stochastic disturbance', *IEEE Transactions on Circuits and Systems II: Express Briefs*, Vol. 66, No. 7, pp.1187–1191.

Ran, M., Wang, Q. and Dong, C. (2016) 'Anti-windup design for uncertain nonlinear systems subject to actuator saturation and external disturbance', *International Journal of Robust and Nonlinear Control*, Vol. 26, No. 15, pp.3421–3438.

Rego, R.C.B. (2019) 'Lpv modeling of boost converter and gain scheduling mpc control', *2019 IEEE 15th Brazilian Power Electronics Conference and 5th IEEE Southern Power Electronics Conference (COBEP/SPEC)*, Santos, Brazil, pp.1–5.

Rego, R.C.B. and Costa, M.V.S. (2020) 'Output feedback robust control with anti-windup applied to the 3ssc boost converter', *IEEE Latin America Transactions*, Vol. 18, No. 05, pp.874–880.

Rego, R.C.B., Costa, M.V.S., Reis, F.E.U. and Bascopé, R.P.T. (2018) 'Análise e simulação do controlador mpc-aw-lmi aplicado ao conversor ccte operando em condições de saturação no sinal de controle', *Congresso Brasileiro de Automática*.

Su, Y., Zheng, C. and Mercorelli, P. (2016) 'Global finite-time stabilization of planar linear systems with actuator saturation', *IEEE Transactions on Circuits and Systems II: Express Briefs*, Vol. 64, No. 8, pp.947–951.

Tarczewski, T., Niewiara, Ł.J., Skiwski, M. and Grzesiak, L.M. (2017) 'Gain-scheduled constrained state feedback control of dc–dc buck power converter', *IET Power Electronics*, Vol. 11, No. 4, pp.735–743.

Tomaszewski, E. and Jiangy, J. (2016) 'An anti-windup scheme for proportional resonant controllers with tuneable phase-shift in voltage source converters', *2016 IEEE Power and Energy Society General Meeting (PESGM)*, IEEE, Boston, MA, USA, pp.1–5.

Turner, M.C., Herrmann, G. and Postlethwaite, I. (2003) 'Discrete-time anti-windup: Part i stability and performance', *European Control Conference (ECC) 2003*, IEEE, Cambridge, UK, pp.473–478.

Wada, N. and Saeki, M. (2016) 'Anti-windup synthesis for a model predictive control system', *IEEJ Transactions on Electrical and Electronic Engineering*, Vol. 11, No. 6, pp.776–785.

Wada, N., Saito, K. and Saeki, M. (2006) 'Model predictive control for linear parameter varying systems using parameter dependent lyapunov function', *IEEE Transactions on Circuits and Systems II: Express Briefs*, Vol. 53, No. 12, pp.1446–1450.

Wan, Z. and Kothare, M.V. (2002) 'Robust output feedback model predictive control using off-line linear matrix inequalities', *Journal of Process Control*, Vol. 12, No. 7, pp.763–774.

Wollnack, S., Abbas, H.S., Tóth, R. and Werner, H. (2017) ' 'Fixed-structure LPV-IO controllers: An implicit representation based approach', *Automatica*, Vol. 83, pp.282–289.

Zheng, C., Su, Y. and Mercorelli, P. (2019) 'Simple saturated relay non-linear pd control for uncertain motion systems with friction and actuator constraint', *IET Control Theory Applications*, Vol. 13, No. 12, pp.1920–1928.

Zheng, H., Zou, T., Hu, J. and Yu, H. (2018) 'An offline optimization and online table look-up strategy of two-layer model predictive control', *IEEE Access*, Vol. 6, pp.47433–47441.

Appendix A. Proof Theorem 2

In order to increase the elasticity of the polytope in the LMI (13) and obtain a faster response of system when the control signal enters the saturation region, the LMI relaxation process will be applied.

The LMI is given by,

$$\begin{bmatrix} -Q_a & * & * & * & * \\ -F_{AW}Q_a & -2U_a & * & * & * \\ 0 & I & -\mu_a I & * & * \\ (C_j + D_j F_{AW})Q_a & D_j U_a & 0 & -I & * \\ (A_j + B_j F_{AW})Q_a & B_j U_a & 0 & 0 & -Q_a \end{bmatrix} < 0. \quad (A1)$$

Since inequalities (A1) hold, defined a matrix $X_a \neq X_a^T$, i.e., the matrices X_{a_j} are non-singular. Letting $X_a(k) = \sum_{j=1}^{l} \mu_j X_{a_j}$ and multiplying to the left of the matrix (A1) by,

$$diag(X_a^T Q_{aj}^{-1}, I, I, I, I) \quad (A2)$$

and from the right by,

$$diag(Q_{aj}^{-1} X_a, I, I, I, I) \quad (A3)$$

inequality (A1) is converted to the form,

$$\begin{bmatrix} -X_a^T Q_{aj}^{-1} X_a & * & * & * & * \\ -F_{AW} X_a & -2U_a & * & * & * \\ 0 & I & -\mu_a I & * & * \\ (C_j + D_j F_{AW})X_a & D_j U_a & 0 & -I & * \\ (A_j + B_j F_{AW})X_a & B_j U_a & 0 & 0 & -Q_{aj} \end{bmatrix} < 0. \quad (A4)$$

Also, recalling that $Q_a(k) = \sum_{j=1}^{l} \mu_j Q_{aj}(k) > 0$ and since,

$$(Q_{aj} - X_a)^T Q_{aj}^{-1}(Q_{aj} - X_a) \geq 0, \quad (A5)$$

gives,

$$-X_a^T Q_{aj}^{-1} X_a \geq -(X_a + X_a^T - Q_{aj}). \quad (A6)$$

Considering the inequality (A6), we have,

$$\begin{bmatrix} -(X_a + X_a^T - Q_{aj}) & * & * & * & * \\ -L_a & -2U_a & * & * & * \\ 0 & I & -\mu_a I & * & * \\ C_j X_a + D_j L_a & D_j U_a & 0 & -I & * \\ A_j X_a + B_j L_a & B_j U_a & 0 & 0 & -Q_{aj} \end{bmatrix} < 0. \quad (A7)$$

where $j = 1, ..., p$, and the gain $F_{AW}(k) = L_a X_a^{-1}$.